Self Assembly of Globular Protein Nanoparticles

Andrey Shiryayev and James D. Gunton

Department of Physics, Lehigh University
Bethlehem, PA 18015

ABSTRACT

A continuum model of the self-assembly of globular protein nanoparticles proposed by Talanquer and Oxtoby (J. Chem. Phys. **109**, 223 (1998)) is investigated numerically, with particular emphasis on the region near the metastable fluid-fluid coexistence curve. The free energy barrier that separates a protein rich metastable fluid phase from its stable crystalline phase is studied for a variety of nucleation pathways in the metastable region. As shown earlier, the nucleation barrier is smallest in the vicinity of the fluid-fluid critical point. An approximate analytic solution is also presented for the shape and properties of the nucleating crystal droplet.

Keywords: nanoparticle, protein, crystallization, nucleation

1 INTRODUCTION

Globular protein molecules provide an excellent example of nanoparticles that can self-assemble to form crystal clusters. The formation of high quality protein crystals is a prerequisite in the determination of the protein structure, which in turn determines protein functions. As a consequence, there is great interest in determining the conditions necessary to form high quality protein crystals. Since nucleation of a crystalline droplet is the critical step toward the formation of the solid phase from the supersaturated solution, this is the focus of current studies. It has been shown that the crystallization of globular proteins can be explained as arising from attractive interactions whose range is small compared with the molecular diameter (corresponding to a narrow window of a small, negative value of the second virial coefficient B_2 [1],[2]). In this case the gas-fluid coexistence curve is in a **metastable** region below the liquidus-solidus coexistence lines, terminating in a metastable critical point (Figure 1). Self-assembling of the globular proteins into nanoscale clusters is a stochastic process which can be characterized by the nucleation rate; this rate is controlled by the free energy barrier between the supersaturated fluid solution and the crystalline state. Talanquer, Oxtoby [3] and ten Wolde and Frenkel [4] shows that the free energy barrier on the path of constant supersaturation is the smallest in the vicinity of the critical point.

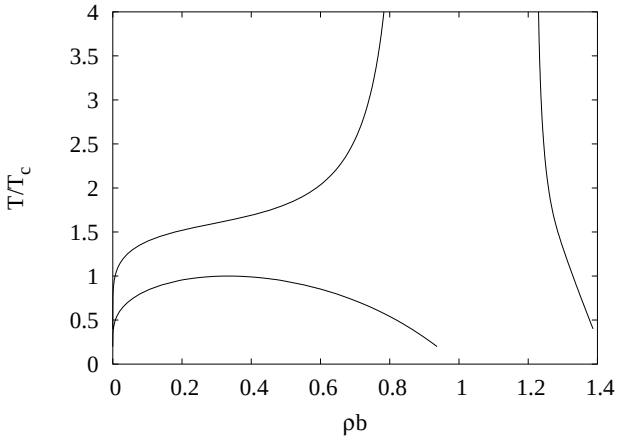

Figure 1: Phase diagram for the nanoparticles with the short-range attraction interactions. The fluid-fluid coexistence curve becomes metastable in this case.

In this work we extend the numerical analysis of a continuum model of globular proteins studied by Talanquer and Oxtoby [3], with particular emphasis on the region near the metastable fluid-fluid coexistence curve.

2 MODEL

We use a model due to Talanquer and Oxtoby [3] to describe globular protein crystallization. Their phase field model is based on the following grand canonical free-energy functional:

$$\Omega[\rho, m] = \int d\vec{r}\Big[f(\rho, m) - \mu\rho + \\ + \frac{1}{2}K_\rho(\nabla\rho)^2 + \frac{1}{2}K_m\rho_s^2(\nabla m)^2\Big] \quad (1)$$

The free energy depends on two order parameters: the (conserved) local density $\rho(\mathbf{r}, t)$ and a (non-conserved) local structural order parameter that shows whether the system is in a solid or fluid phase $m(\mathbf{r}, t)$. Here $f(\rho, m)$ is the Helmholtz free-energy density and μ is the chemical potential. Talanquer and Oxtoby [3] use the van der Waals free energy density for the fluid branch:

$$f_f(\rho, m) = k_B T \rho \left[\ln \rho - 1 - \ln(1 - \rho b)\right] - a\rho^2 + k_b T \alpha_1 m^2 \quad (2)$$

and a corresponding van der Waals free energy for the solid phase:

$$f_s(\rho, m) = k_B T \rho \left[\ln \rho - 1 - \ln(1 - \bar{\rho} b)\right] - (a + a_m m_s^2)\rho^2 + k_b T(\alpha_1 m^2 + \alpha_2) \quad (3)$$

Here $\bar{\rho}$ plays a role of a weighted coarse grained density $\bar{\rho} = \rho(1 - \alpha_3 m(2 - m))$ where the term in square brackets implements a difference between the fluid and solid close-packing limits. For the fluid close-packing limit, $\rho b = 1$, while for the solid close-packing limit $\bar{\rho} b = 1$. The quantity $m_s(\rho)$ is the equilibrium value of the order parameter in the solid phase and hence is a solution of the equation $(\partial f_s/\partial m)_{m_s(\rho)} = 0$. Thus in the solid close-packing limit ($b\bar{\rho} = 1$) $m_s = 1$. The parameter a_m in equation (3) has been introduced in order to change the range of the attractive interactions between molecules in the solid phase from that in the liquid phase (as described by the parameter a in equation (2)).

The chemical potential in the solid and fluid phases is the first derivative of the free energy with respect to density: $\mu = (\partial f/\partial \rho)_T$. In order to get coexisting densities ρ_α and ρ_β we have to solve the equations $\mu(\rho_\alpha) = \mu(\rho_\beta)$ and $\omega(\rho_\alpha) = \omega(\rho_\beta)$, where $\omega = f - \mu\rho$. Graphically this gives the well-known "common tangent" rule for coexistence. By repeating this for different temperatures we can obtain the entire phase diagram.

In order to obtain a critical droplet profile we must solve the Euler-Lagrange equations with appropriate boundary conditions:

$$\frac{\delta\Omega}{\delta\rho} = 0 \quad \text{and} \quad \frac{\delta\Omega}{\delta m} = 0$$

i.e.,

$$-K_\rho \nabla^2 \rho + \frac{\partial f}{\partial \rho} - \mu = 0 \quad (4)$$

$$-K_m \nabla^2 m + \frac{\partial f}{\partial m} = 0 \quad (5)$$

Using the solutions of (4) for $\overline{\rho}(\mathbf{r})$ and $\overline{m}(\mathbf{r})$ we can obtain such properties of the inhomogeneous system as the free energy barrier and the surface tension.

3 NUMERICAL RESULTS

Here we present some results, extending the work of [3], for the following choice of parameters: $a = 1$, $b = 1$, $\alpha_1 = 0.25$, $\alpha_2 = 2$, $\alpha_3 = 0.3$, $a_m = 1$. The phase diagram for these values is shown in Figure 1, which shows in particular a metastable fluid-fluid coexistence curve. The existence of the metastable critical point affects the nucleation and growth processes in the vicinity of this point.

The main quantity characterizing the self-assembly process is a nucleation rate I, given by

$$I = I_0 e^{-\Delta\Omega/kT} \quad (6)$$

where I_0 is a prefactor given by the product of dynamical and statistical parts [6]. To be able to control the self-assembly process we need to understand how this metastable critical point affects nucleation. We calculate the free energy barrier for different thermodynamic paths. (Some results for this barrier were presented in [3] and in [5].) The barrier dependence on temperature and density in the metastable region between the liquidus (solubility curve) and solidus lines is quite straightforward. As we increase the temperature at the constant density of the disordered state the barrier increases and diverges at liquidus line. The same behavior is obtained [5] if we decrease the density of the disordered state an the constant temperature. This is because at any point on the solubility curve the free energy is infinite and decreases as one moves away from it and vanishes at the spinodal.

However, the existence of the metastable fluid-fluid coexistence curve changes the pathways of the constant free energy barrier and constant supersaturation lines as compared with the case in which the coexistence curve is not metastable. We can also see that along the lines with constant supersaturation the free energy barrier decreases as one approaches the critical point (Fig. 2), which is consistent with [3]. Figure 2 shows that the free energy barrier has a minimum near, but not at, the critical point. The location of this minimum changes from above the critical point for low supersaturation to below the critical point for high supersaturation. It also can be seen that the increase of the free energy barrier below the critical point becomes very sharp for the cases where the constant supersaturation lines intersect the fluid-fluid coexistence curve. Because there is a discontinuity in those lines of constant supersaturation which intersect the fluid-fluid coexistence curve, the free energy barrier has a corresponding discontinuity. this leads to the jumps in the dependence of the barrier on temperature (fig. 2 for $\Delta\mu = 0.8$ and $\Delta\mu = 0.9$.). As we can see from figure 3 the surface tension also has a discontinuity at $\Delta\mu = 0.8$ and $\Delta\mu = 0.9$. In order to understand the behavior of the free energy barrier along the constant supersaturation lines, we first consider their shape. At high temperatures these lines are more vertical (constant density lines) and the free energy barrier decreases with temperature. Near the critical

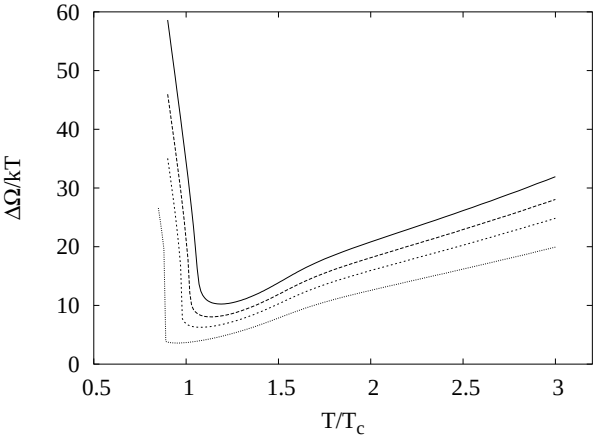

Figure 2: Dependence of the free energy barrier versus temperature at constant supersaturation. From top to bottom $\Delta\mu = 0.7$, 0.75, 0.8, 0.9.

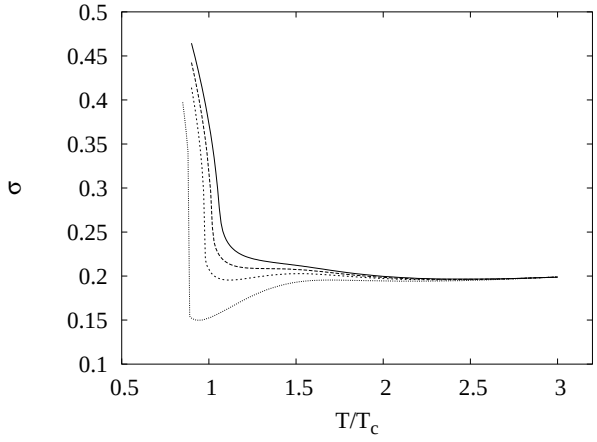

Figure 3: Dependence of the surface tension versus temperature at constant supersaturation. From top to bottom $\Delta\mu = 0.7$, 0.75, 0.8, 0.9.

point the curves become almost horizontal (isothermal lines) and the barrier starts to increase. Thus the shape of the constant supersaturation curve in some sense determines the behavior of the free energy barrier. To understand this in more detail, we note that the derivative of temperature with respect to density at constant supersaturation is

$$\left(\frac{\partial T}{\partial \rho_0}\right)_{\Delta\mu} = -\frac{\left(\frac{\partial \Delta\mu}{\partial \rho_0}\right)}{\left(\frac{\partial \Delta\mu}{\partial T}\right)} = -\left[\frac{f^{(f)}_{\rho\rho}}{\left(\frac{\partial \Delta\mu}{\partial T}\right)}\right]_{\rho=\rho_0} \tag{7}$$

where $f_{\rho\rho}$ is evaluated at the background fluid density. This derivative vanishes at the critical point, so that the constant supersaturation lines become horizontal in the vicinity of the critical point. On the other hand, at large temperatures the denominator vanishes, so that the constant supersaturation lines become vertical. Thus we see that the presence of the critical point changes the behavior of the free energy barrier from decreasing as we lower the temperature far from the critical point (the vertical part of the $\Delta\mu = const$ lines) to increasing as we lower the temperature to its critical value (the horizontal part of the $\Delta\mu = const$ lines). Therefore somewhere in between there is a minimum of the free energy barrier. Thus we can conclude that the free energy barrier is relatively unaffected by the existence of the critical point along paths of constant temperature or constant density , whereas it plays a crucial role along paths of constant supersaturation

One quantity of interest is the excess number of molecules, defined as the number of molecules in the presence of the droplet relative to the number of molecules in the spatially homogeneous metastable state:

$$N = \int_V (\rho(r) - \rho_0) d\vec{r} \tag{8}$$

We can calculate the number of molecules in the crystalline state using $m(r)$, since this phase field shows whether a point is in the solid or fluid state. Thus:

$$N_c = \int_V m(r)(\rho(r) - \rho_0) d\vec{r} \tag{9}$$

Mean field theory yields a divergence in the excess number of particles at the metastable critical point, whereas the number of particles in the crystalline state remains finite. We can check our numerical results with the nucleation theorem [7], [8]:

$$\frac{\partial \Delta\Omega}{\partial \Delta\mu} = -N \tag{10}$$

Thus we can take a derivative of the free energy barrier with respect to supersaturation and compare this with our results for the dependence of the excess number of particles on the supersaturation [5]. We see that the free energy barrier decreases rapidly near the critical point as a function of the supersaturation. This happens because the background fluid density as a function of the supersaturation becomes flat in the vicinity of the critical point.

4 DISCUSSION AND CONCLUSIONS

In this paper we have extended the numerical results [3] to obtain a better understanding of nucleation for their model. In particular, we have calculated the density and structure order parameter profiles of the critical nucleating droplet for different temperatures at constant supersaturation. This solution of the saddle

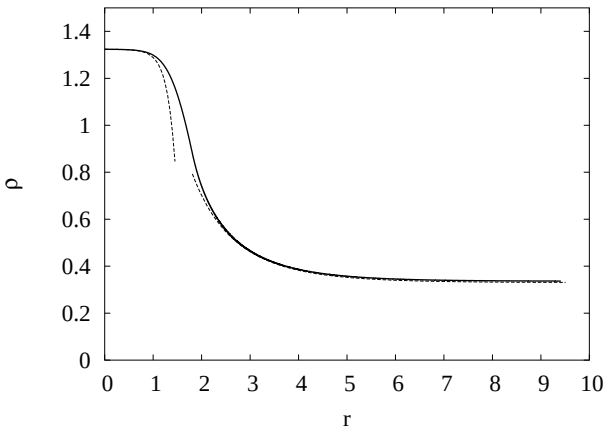

Figure 4: Comparison of the numerically obtained density profile (at $T/T_c = 1.2$ and $\rho_0 = 0.33$) with the tail and core approximations (dashed lines).

point equations then yields the free energy barrier to nucleation and the surface tension. As it can be seen the nucleation barrier has a minimum near the critical point. Also if the path with constant $\Delta\mu$ crosses fluid-fluid coexistence curve, then both free energy barrier and surface tension have discontinuity.

In our previous paper [5] we also presented analytical approximation for the core and the tail of the critical cluster. The tail solution is in agreement with Sear's approximation [9]. Figure 4 shows these approximation in comparison with numerical solution. We can see, that while the core approximation is very close to the numerical solution near the center of the droplet it diverges quickly as it approaches the interface region.

This work was supported by NSF grant DMR-0302598.

REFERENCES

[1] A. George and W. Wilson, Acta Cryst. D **50**, 361 (1994).
[2] D. Rosenbaum, P. C. Zamora, and C. F. Zukoski, Phys. Rev. Lett. **76**, 150 (1996).
[3] V. Talanquer and D. Oxtoby, J. Chem. Phys. **109**, 223 (1998).
[4] P.R. ten Wolde and D. Frenkel, Science **277**, 1975 (1997).
[5] Andrey Shiryayev and James D. Gunton J. Chem. Phys. to be published.
[6] J. Langer, Annals of Physics **54**, 258 (1969).
[7] D. Kashchiev, J. Chem. Phys. **76**, 5098 (1982).
[8] Y. Viisanen, R. Strey, and H. Reiss, J. Chem. Phys. **99**, 4680 (1993).
[9] R. Sear, J. Chem. Phys. **114**, 3170 (2001).